Dependence of Secondary Electron Emission upon Angle of Incidence of 1.3-Mev Primaries*

R. A. SHATAS, J. F. MARSHALL, AND M. A. POMERANTZ
Bartol Research Foundation of The Franklin Institute, Swarthmore, Pennsylvania
(Received January 19, 1956)

Utilizing a high-energy beam and targets sufficiently thin to permit the primary electrons to pass through with negligible scattering and energy loss, the secondary electron yield has been observed to vary with the angle of incidence of the primaries in accordance with the relationship $\delta(\theta)=\delta_0 \sec\theta$. This angular dependence is predicted theoretically on the basis of the single assumption that the secondary electrons can be treated as though they were produced with an isotropic velocity distribution. At large angles of incidence, the variation is slightly greater as a consequence of scattering effects which are larger in Ni than in an approximately equal thickness in mg cm^{-2} of Al. The experimentally observed equality of the yields in the forward and backward directions is consistent with the conclusion that the angular distribution of the secondaries is effectively isotropic.

I. INTRODUCTION

It is a well established fact that the yield of secondary electrons emitted from a solid target rises as the angle of incidence of the primary electron beam is increased.[1,2] Qualitatively, the phenomenon is readily explained in terms of the decreased path which secondaries produced at a given point along the trajectory of the obliquely incident primary must traverse to reach the surface. Various theoretical expressions relating the yield to the angle of incidence have been proposed.[3,4] However, owing to the complexities of the processes involved when the primary energy is low,[5] as has been the case in all of the previous investigations of this subject ($V_p<2500$ v), somewhat questionable simplifying assumptions have been invoked in the derivation of these expressions.

The situation becomes much simpler when the primaries are extremely energetic and the targets are sufficiently thin to permit the bombarding electrons to pass through with negligible scattering and energy loss. Under these conditions, the rate of production of secondaries is constant along the entire rectilinear path of a primary electron, and it is not necessary to make any arbitrary assumptions regarding the nature of the absorption process or the "average" depth of production of secondaries. The "sandwich" arrangement,[6] which has been utilized in various investigations of secondary emission produced by 1.3-Mev electrons from a multiple-cavity linear accelerator, is readily adaptable to measurements of the yield as a function of primary angle of incidence under the desired conditions.

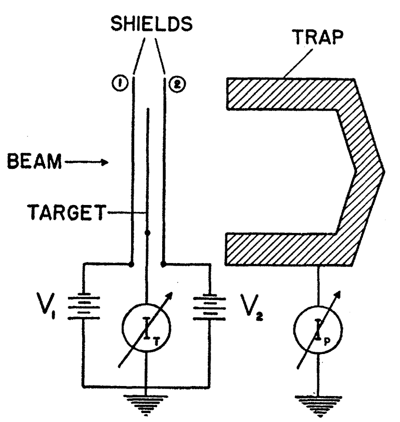

FIG. 1. Schematic diagram of "sandwich" arrangement utilized for measurements of secondary electron emission produced by high-energy primaries.

II. EXPERIMENTAL PROCEDURE

A. Method

The method of measurement is indicated schematically in Fig. 1. The analyzed beam from the linear accelerator passes through a carbon collimator, then through the sandwich arrangement consisting of the target and two thin foil shields, and is finally stopped by the carbon trap. The yield from face 1 can be determined from observations of the current $I_T(V_1)$ corresponding to two alternative sets of electrode potentials. Thus, if the shield 2 is maintained at an arbitrary constant voltage, V_2, the measured target current I_T is given by

$$I_T(V_1<0)=T_1(>V_1)-S_1+A_2, \quad (1)$$

$$I_T(V_1=0)=T_1-S_1+A_2, \quad (2)$$

where $T_1(>V_1)$ represents the current of secondary electrons leaving the target from face 1 with a normal velocity component sufficient to overcome the retarding potential V_1, and S_1 is the current of secondary electrons reaching the target from the shield opposite face 1. When the potential difference between face 1 and the opposite shield is zero, all of the secondaries from each surface reach the other in accordance with Eq. (2). Inasmuch as V_2 is unchanged, the term A_2 representing the contribution to I_T by electrons flowing to or from face 2 is constant. The net current of second-

* Assisted by the Office of Ordnance Research, U. S. Army.
[1] H. Bruining, Physica 3, 1046 (1936).
[2] H. O. Müller, Z. Physik 104, 475 (1937).
[3] H. Bruining, Physica 5, 901 (1938).
[4] S. J. Lukjanov, Physik Z. Sowjetunion 13, 123 (1938).
[5] M. A. Pomerantz and J. F. Marshall, Proc. Inst. Radio Engrs. 39, 1367 (1951).
[6] Pomerantz, Marshall, and Shatas, Phys. Rev. 95, 633 (1954).

ary electrons leaving face 1 with energies below that required to overcome the retarding potential V_1 is obtained by subtracting Eq. (1) from Eq. (2). The yield from face 2 is determined by a similar procedure. The secondary emission of the inner surfaces of the two shields can also be deduced from measurements of $I_T(V_n>0)$ by invoking the corresponding relationships.

If all of the surfaces inside the sandwich are identical, the effects which would be introduced by the existence of contact potentials are avoided. Furthermore, if, in addition, the three foil thicknesses are equal so that the delta-ray[7] yields from shields and target do not differ, the target current when all three electrodes are at the same potential is

$$I_T(V_1=0,\quad V_2=0)=T_1-S_1+T_2-S_2=0. \qquad (3)$$

This provides a method for detecting any possible difference in surface conditions, since under ideal conditions all yields are equal.

B. Tube Design

The manner in which the target is mounted in the experimental tube is shown in Fig. 2. The sandwich components are as large as possible (>1 in.×1 in.) and the target-shield spacing is as small as possible (<0.08 in.) in accordance with certain geometrical considerations. The maximum angle at which satisfactory measurements are feasible is approximately 72° with the present arrangement.

The shields prevent stray secondary electrons from the graphite collimator and trap from striking the target. The sandwich is supported by a rod attached to a sleeve. An O-ring seal permits rotation with respect to a fixed side-tube (not illustrated) which is perpendicular to the plane of the diagram. Relative angles can be read off an inscribed scale to within 0.5° and normal incidence is determined visually with an uncertainty of about 2°. The sandwich is retractable to permit measurement of the trap current with the foils removed from the beam in order to ascertain whether any appreciable fraction of the primary electron current does not reach the trap when the foils are interposed.

The demountable tube is attached to the magnetic spectrum analyzer at the output end of the linear accelerator[8] and is pumped by the same vacuum system.

C. Determination of Yields

Both the target and trap currents are measured simultaneously by two integrating micromicroammeters. The potential of each shield (V_1 and V_2) can be set independently at 0, $+V$ or $-V$ volts with respect to the target. The value of V chosen, $|V|=30$ volts, is sufficiently high to repel all of the low-energy secondaries from the negatively charged electrode.[9]

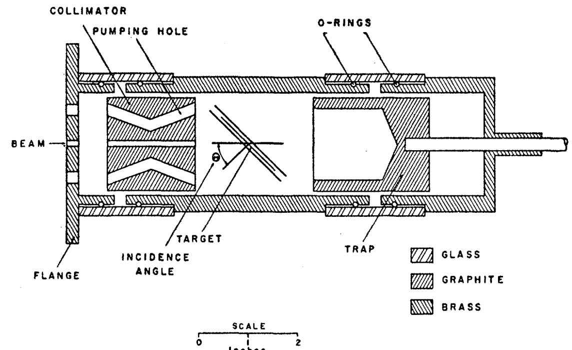

FIG. 2. Demountable experimental tube. Support assembly (not shown) permits rotation of sandwich and retraction from the beam.

Under these conditions, nine individual combinations of shield potentials V_1 and V_2 are possible. Accordingly, at each incidence angle the target current is measured once for each different combination of V_1 and V_2.

The yield from face 1, for example, is then determined by averaging the three values computed from Eqs. (1) and (2) on the basis of the measurements of $I_T(V_1)$ corresponding to each of three different potentials of the opposite shield ($V_2=0$, -30, $+30$ volts). The agreement among these three values indicates that extraneous low energy electrons from outside the sandwich system do not reach the target electrode.

By an analogous procedure, the yields from both shield electrodes can also be determined. This provides a method for checking the internal consistency of the measurements. The corresponding shield and target data were always in good agreement.

The sandwich assembly can be raised or lowered into the path of the primary beam by remote control during the measurement of the trap current. At incidence angles below 60° and 75° for the nickel and aluminum sandwiches, respectively, no change in the trap current is observed. Thus, up to these limits, large-angle scattering and back scattering of primaries is negligible, and the trap current reading when the sandwich assembly is interposed in the path of the beam represents the true intensity of the incident primary beam.

D. Targets

Commercially-available 2-mg/cm² aluminum foils were used in the aluminum target assembly which consisted of a 1 in.×1 in. target sandwiched between two $1\frac{1}{4}$-in. square shields. These were prepared by wrapping the edge of the foil cut-outs around flattened 0.020-in. nickel wire squares which served as supporting structures.

The nickel sandwich was fabricated with 2.5-mg/cm² foil of commercial purity in a similar manner, except that the sizes of the target and the shields were increased to 1 in.×$1\frac{3}{4}$ in. and $1\frac{1}{4}$ in.×2 in., respectively.

[7] Marshall, Shatas, and Pomerantz, Phys. Rev. **95**, 634 (1954).
[8] Shatas, Marshall, and Pomerantz, Phys. Rev. **96**, 1199 (1954).
[9] Shatas, Marshall, and Pomerantz, Phys. Rev. **94**, 757 (1954).

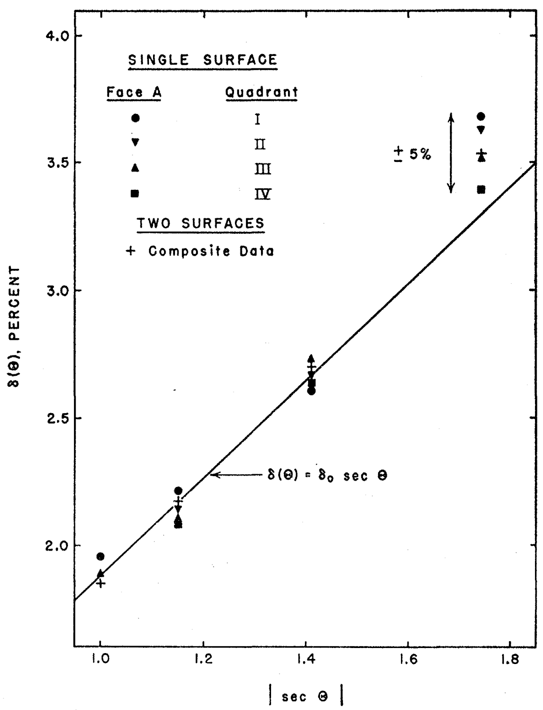

FIG. 3. Yield, $\delta(\theta)$, [current of low-energy secondary electrons emitted from single face per unit primary current] plotted as a function of the absolute value of sec θ for 2.5 mg/cm² Ni target.

Immediately prior to mounting in the experimental tube, the sandwich was cleaned with ethanol and acetone. Because the secondary emission tube communicates directly with the vacuum system of the accelerator, the pressure during the measurements is approximately 5×10^{-6} mm of Hg. However, in view of the fact that the secondary electron yields from the target and both shields do not vary with time throughout the course of the experiment, it is safe to assume that the nature of the surfaces remains unchanged. On the other hand, extreme cleanliness of the surfaces is not required in measurements of the dependence of secondary emission upon primary incidence angle, inasmuch as the absolute yields are not involved.

III. RESULTS

A. Nickel

Typical data obtained with a nickel target are shown in Fig. 3, where the yield is plotted as a function of the secant of the primary incidence angle. The consistency among the points for a specific face in all four quadrants attests to the uniformity of the surface and the absence of any significant variations which might be introduced by shifts in the position of the bombarded area as the target is rotated. Points for the other face are indistinguishable from those plotted. The experimental uncertainty of 5% in the individual values arises from short-period fluctuations in the primary beam intensity. The straight line representing the function $\delta(\theta)=\delta_0 \times|\sec\theta|$, where δ_0 is the yield at normal incidence, is drawn to fit the composite points (+, average of values for both faces in four quadrants) at small angles. When θ exceeds approximately 50°, the experimental points lie somewhat above the extrapolated $\delta_0 \sec\theta$ curve.

B. Aluminum

The data for aluminum are plotted in Fig. 4. In this series, a shift in the angular readings was necessitated by the fact that the fiducial index differed from the true angle by 1°40′. This constant angular phase difference was determined by plotting the yield as a function of the indicated angle (rather than secθ), and shifting the smooth curve through the data for Quadrants 1 and 2 to overlap the similar curve for Quadrants 3 and 4. As a consequence of this zero calibration procedure, the measurements at each nominal angle actually correspond to two slightly different angles.

The agreement among the points for both faces in all quadrants indicates the absence of disturbing effects attributable to geometrical factors or nonuniform surface conditions. The departure from the empirical secθ dependence is detectable above 65°, a considerably larger angle than with the nickel target.

IV. DISCUSSION

The theoretical analysis of the dependence of secondary electron yield upon the angle of incidence of

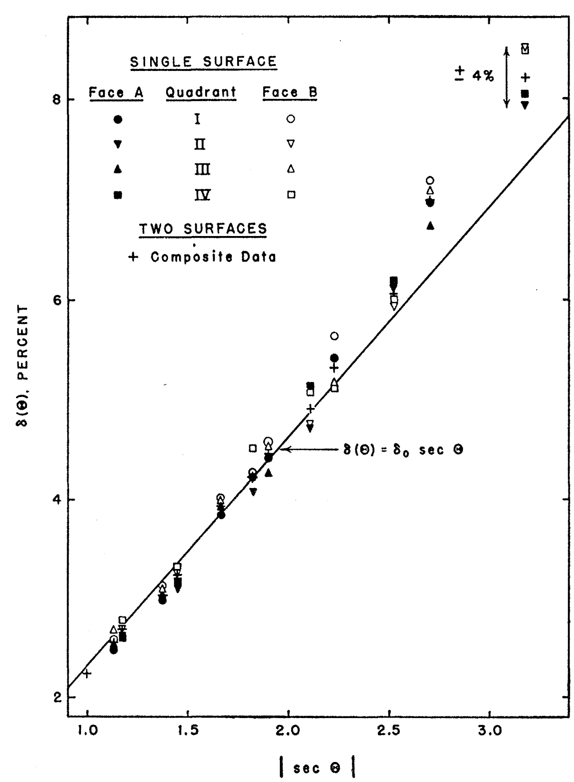

FIG. 4. Plot of data obtained with 2.0-mg/cm² Al target.

the primaries is quite straightforward when the range of the latter greatly exceeds that of the secondaries. In this case, it is necesasary to assume only that the secondary electrons can be treated as though they were produced with an isotropic velocity distribution. The expression for the secondary yield, δ, from a given face of the target is then

$$\delta=\int_0^\infty N(l)p(x)dl, \tag{4}$$

where $N(l)$ is the number of secondaries produced per unit path of the primary, and $p(x)$ is the probability that a secondary produced at a distance x from the surface of the solid will escape. The distance l is measured along the path of the primary electrons.

It should be remarked that the assumption of an isotropic distribution of the secondaries does not imply that they are actually emitted isotropically in the initial primary interaction, but rather that, as a consequence of scattering processes with a mean free path which is short compared with x, the secondaries effectively diffuse to the surface from the point of origin.

In the present experiments, the high-energy primary electrons suffer negligible energy loss in traversing the region for which the escape probability of the secondaries is appreciable,[10] hence the rate of production of secondaries is essentially constant along l. Consequently, Eq. (4) becomes

$$\delta=N(0)\int_0^\infty p(x)dl. \tag{5}$$

As is evident in Fig. 5,

$$l=x\sec\theta, \tag{6}$$

and

$$\delta=N(0)\sec\theta\int_0^\infty p(x)dx. \tag{7}$$

The integration can be extended to infinity because $p(x)$ is a rapidly decreasing function. Since neither $N(0)$, the production rate at the surface, nor the integrand depend upon θ, the yield at normal incidence ($\theta=0°$) is given by

$$\delta(0)=N(0)\int_0^\infty p(x)dx, \tag{8}$$

and Eq. (7) becomes

$$\delta(\theta)=\delta(0)\sec\theta. \tag{9}$$

Thus, for high-energy primaries, the secondary yield will be proportional to the secant of the angle of

[10] Actually, the primary electrons suffer negligible energy loss in traversing the entire target thickness. However, the general theory developed here would be applicable even if this were not the case, providing the energy is constant throughout the region in which most of the emitted secondaries are produced.

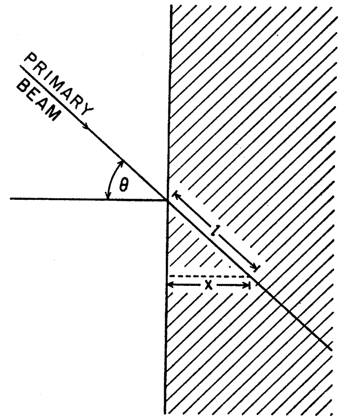

FIG. 5. Dependence of path traversed by escaping secondaries upon angle of incidence of primary beam.

incidence, if the distribution of secondary velocities is essentially isotropic. Furthermore, if this assumption is not valid, the secant law should not be expected to hold, since only very special velocity distributions would lead to this simple result.

In the experiments described here, the yield follows the secant law up to angles of the order of 65° for Al, thereby confirming the validity of the above hypotheses. At higher angles of incidence, the angular dependence is somewhat greater than predicted by Eq. (9). These deviations at steep angles are expected to occur as a consequence of the fact that the primaries are slightly scattered by the first foil of the sandwich, and hence strike the target at a variety of angles distributed about the measured angle of incidence. This scattering results in an effective incidence angle which is somewhat higher than that measured and consequently gives rise to a more rapid increase in yield. In view of the fact that the mean square scattering angle varies as Z^2, the departure from the $\sec\theta$ law with a nickel target should occur at a smaller angle than with an approximately equal thickness (expressed in mg/cm^2) of aluminum. As noted in the previous section, this is confirmed experimentally. Deviations at large angles can also be introduced by geometrical effects and by small wrinkles in the target foil.

These experiments reveal that the law given by Eq. (9) is valid and that the single assumption required for its derivation is essentially correct, thus establishing that the angular distribution of secondary electron velocities is effectively isotropic. The observation of equality of yields in the forward and backward directions also confirms the absence of any assymmetry in the distribution of secondary electrons about the plane perpendicular to the direction of motion of the primary beam. However, the fact that the front-back yield ratio is unity does not specifically constitute evidence that the distribution is isotropic. On the other hand, if the yield for one face exceeded that from the other because of a preferred direction of motion of secondaries, the secant law would not apply.

Actually, any departure from equal yields in the two

directions introduced solely by scattering in the target should be accompanied by a deviation from the secant law for the exit face. With the present arrangement in which the foils are identical, the departure from the secant law for the surface in the forward direction (Fig. 1, face 2) should be twice that for the entrance face. Since this is not precisely verified experimentally, some of the other factors mentioned above undoubtedly influence the measurements at large angles to some extent.

It should be emphasized that the situation is much more complicated when the bombarding energies are low. In that case, the range of the primary electrons is not large compared with the range of the secondaries, and the rate of production, $N(l)$, is a very sensitive function of l. Under these circumstances, the theoretical problem becomes much more difficult and the yield should certainly not be expected to follow a simple secant law.

V. ACKNOWLEDGMENTS

It is a pleasure to acknowledge the assistance of Mr. Arthur E. Smith in the performance of these experiments.

PHYSICAL REVIEW VOLUME 102, NUMBER 3 MAY 1, 1956

Field-Induced Color Shift in Electroluminescent Zinc Sulfide*

JOHN F. WAYMOUTH, *Sylvania Electric Products Incorporated, Salem, Massachusetts*

AND

FRANCIS BITTER,† *Massachusetts Institute of Technology, Cambridge, Massachusetts*

(Received November 23, 1955)

In a previous paper it was shown that the application of an electric field to certain electroluminescent phosphors in an equilibrium condition produced little light, but that luminescent centers were activated in some way, and radiated upon removal of the field. It is here shown that while the liminescent centers are held in the activated state, changes are taking place which are observed as a color shift in the light radiated as a function of time held in the activated state. For certain green and blue phosphors, prompt removal of the field after activation produces green and blue bands which are also observed in operation at 60 cps. If the field is maintained for some seconds, and then removed, these bands are suppressed and a "yellow band" appears in their place at a rate determined by a temperature dependent time constant of the order of a second at room temperature. Possible explanations of this result are discussed.

IN an article[1] recently published in this journal experiments are described concerning the response of electroluminescent cells to the application and removal of dc fields. The purpose of this paper is to report on additional experiments which reveal additional detail concerning the mechanisms involved.

The procedure previously[1] adopted, and elaborated here, begins with the phosphor sample in a condition which may be referred to as "zero-field equilibrium." This condition is arrived at either by allowing the sample, a thin sheet of plastic in which the phosphor is imbedded, to remain in zero applied field in the dark for some hours, or by irradiating the sample for some seconds with infrared light in zero applied field. If a dc field is applied, and then removed a few seconds later, it is observed that the integrated light output on charging the sample condenser (ILO_c) is of the order of one percent of the integrated light output on discharging the sample condenser (ILO_d).

The light output on discharging (ILO_d) decreases with increasing time t during which the sample condenser was charged. The light output observed on recharging the sample condenser (ILO_c) which has been charged for a length of time t depends upon both the charging time t and the time t' between discharging and recharging. For fixed t', ILO_c increases with increasing t toward a saturation value approximately equal to ILO_d for t very small. For a fixed value of t, ILO_c decreases with increasing discharged time t' toward its zero-field equilibrium value. These observations have all been qualitatively explained by the hypothesis that when the electric field is applied, a "frozen" polarization develops, which eventually reduces the actual field in the phosphor to zero.[1] The time constants of these effects are of the order of fifty to one hundred seconds.

The new experiments to be described below relate to the emission spectrum of these ILO's. It had been noted that ILO_c was "bluer" than ILO_d but that ILO_c had approximately the same emission spectrum as the 60-cps luminescence.[2] Moreover, the emission

* This material was first presented at the Centennial Symposium on Electroluminescence and Photoconduction in Inorganic Phosphors at the Polytechnic Institute of Brooklyn, September 9 and 10, 1955.

† This work was done at the Sylvania Electric Products, Inc., plant in Salem, Massachusetts.

[1] J. F. Waymouth and F. Bitter, Phys. Rev. 95, 941 (1954).

[2] J. F. Waymouth, J. Electrochem. Soc. 100, 81 (1953).